Shear force control for a terahertz near field microscope

F. Buersgens and G. Acuna
Photonics and Optoelectronics Group, University of Munich, Amalienstr. 54, 80799 Munich, Germany and Center for Nanoscience, University of Munich, Geschwister-Scholl-Platz 1, 80539 Munich, Germany

C. H. Lang and S. I. Potrebic
Photonics and Optoelectronics Group, University of Munich, Amalienstr. 54, 80799 Munich, Germany

S. Manus
Center for Nanoscience, University of Munich, Geschwister-Scholl-Platz 1, 80539 Munich, Germany

R. Kersting
Photonics and Optoelectronics Group, University of Munich, Amalienstr. 54, 80799 Munich, Germany and Center for Nanoscience, University of Munich, Geschwister-Scholl-Platz 1, 80539 Munich, Germany

(Received 25 May 2007; accepted 6 October 2007; published online 2 November 2007)

We report on the advancement of apertureless terahertz microscopy by active shear force control of the scanning probe. Extreme subwavelength spatial resolution and a maximized image contrast are achieved by maintaining a tip-surface distance of about 20 nm. The constant distance between scanning tip and surface results in terahertz images that mirror the dielectric permittivity of the surface. © *2007 American Institute of Physics.* [DOI: 10.1063/1.2804077]

I. INTRODUCTION

The recent developments in terahertz technology promise applications in a variety of fields such as material science, semiconductor technology, or the nanosciences in general. The broad applicability results from the fact that many chemical compounds, semiconductor structures, or nano-objects exhibit infrared active resonances in the terahertz range. Furthermore, scattering occurs in many solids at terahertz rates. Therefore, terahertz techniques are an ideal tool for contactless characterization. Examples are the tracking of gases by their far-infrared absorption lines,[1,2] the identification of organic substances by their vibrational modes,[3,4] the measurement of the Drude conductivity in semiconductors,[5] or the time-resolved dynamics of intersubband transitions.[6]

The pioneering works on terahertz imaging paved the way for obtaining two-dimensional[7–9] and even three-dimensional images[10] of dielectric material properties. Most of these approaches are far field techniques and their spatial resolution is limited by the Abbe-Rayleigh criterion to about the wavelength size. Such resolutions are not sufficient for characterizing individual state of the art semiconductor devices or even nano-objects. One possibility to achieve much finer resolutions is scanning a subwavelength aperture across the sample.[11–13] Although resolutions down to 7 μm were demonstrated, the drawback of apertures is that their light transmission decreases with the sixth power of the aperture's diameter.[14] Attractive alternatives for achieving ultrafine resolutions are apertureless techniques[15–17] where the radiation field is focused by a metal probe. Recently, apertureless approaches were demonstrated for the terahertz range[18] where the antenna properties of the probe allow for extreme subwavelength resolution.[19–21] Spatial resolutions down to 150 nm were achieved in terahertz apertureless near field scanning optical microscopy (THz-ANSOM).[22]

Despite the extreme subwavelength resolutions that can be obtained by apertureless terahertz microscopy, the application of the technique is hindered by the requirement that the sampling tip has to be held in close proximity to the surface.[19] This results from the finding that for submicrometer resolutions, the tip-surface distance has to be smaller than 100 nm.[23,24] Additionally, it was observed that the image contrast decreases significantly with tip-sample separation.[24] These requirements make terahertz microscopy experimentally challenging, in particular, on soft objects, which can easily be destroyed by the metal tip. One way of circumventing this problem is to keep the needle at a height larger than the topographic roughness of the sample. However, this reduces the image contrast and deteriorates the resolution. Variations in the topographic profile $\Delta z(x,y)$ cause changes in the amount of the dielectric material sensed by the needle and therefore contribute to the image contrast. This makes it impossible to deduce the sample's dielectric permittivity $\epsilon(\omega,x,y)$ from the image data.

The ambiguity due to the sample topography can be avoided if the distance between tip and surface is held constant, ideally on a nanometer scale. This could be achieved with a scanning tunneling microscope (STM), where the exponential dependence of the tunneling current on the probe-sample separation allows for very accurate distance control. However, many samples of interest are nonconductive and are therefore not accessible via such an approach. Alternatively, scanning force techniques as used for atomic force microscopy (AFM) appear attractive. However, terahertz microscopy requires rather macroscopic metallic probes with a length of several millimeters. Thus, standard AFM cantilevers are inappropriate for this purpose.

For controlling the tip-surface distance, we adapted a technique that measures the shear force between the probe tip and the surface.[25–27] This concept is used in shear force

microscopy (SFM) where subatomic resolutions have been demonstrated.[28] In this contribution, we present the implementation of shear force techniques for THz-ANSOM, which allows us to maintain a constant nanometer distance between the sampling tip and the surface. We will show that the technique provides extreme subwavelength resolutions, high image contrast, and a strongly enhanced reliability. In previous works,[19,22] the image contrast resulted from the topography of the structure, as well as from the dielectric contrast, which limits quantitative interpretations of terahertz images. The scientific advancement of shear force controlled terahertz microscopy is that sample areas with different high-frequency dielectric permittivity $\epsilon(\omega,x,y)$ can be distinguished. Terahertz micrographs recorded at a constant distance between sampling tip and surface mirror exclusively the dielectric properties of the surface.

In the following section, we describe the experimental technique and technical details required for terahertz microscopy. Experimental results are described in Sec. III and the advantages of shear force controlled terahertz microscopy are summarized in Sec. IV.

II. EXPERIMENTAL TECHNIQUE

A. Terahertz microscopy

The terahertz radiation is generated by femtosecond laser pulses of a commercial Ti:sapphire laser (Mai-Tai, Spectra Physics). It delivers 60 fs pulses of 13 nJ energy, centered around a wavelength of 780 nm, at a repetition rate of 80 MHz. About 700 mW are used to excite an InAs crystal n doped at $N_D=2\times10^{16}$ cm^{-3}. The impulsive excitation initiates plasma oscillations of the extrinsic carriers in the InAs. Their coherent oscillation leads to the emission of few-cycle terahertz pulses.[29,30] The pulse shape depends only weakly on the excitation density. A typical transient of the electric terahertz field transmitted through the microscope is shown in Fig. 1(a). The spectral composition and the amplitude of the transmitted radiation change with the tip-surface separation. Figure 1(b) shows the differential near field spectra[31] for the respective tip-surface distances as well as a reference spectrum of the impinging terahertz field.

The terahertz pulses are time resolved by electro-optic sampling in a 1 mm thick (110) ZnTe crystal.[32] The laser pulses that probe the terahertz beam in the ZnTe crystal are detected by balanced photodiodes and standard lock-in techniques. Signal to noise ratios of 2×10^4 $\sqrt{\text{Hz}}$ are obtained.

For microscopy, the terahertz beam is fed into the microscope head, which is shown schematically in Fig. 2. Parabolic mirror optics (numerical aperture $\approx$0.16) focus the incident radiation onto the sample to a diffraction limited spot with a diameter of $D\approx4\lambda$. Only the radiation that is transmitted in specular direction is collected for time-resolved detection in the ZnTe crystal. Spatial resolution is achieved by the tungsten tip, which is placed above the center of the focus. It concentrates a fraction of the incident radiation field to a spot on the surface that is comparable to its apex (illustrated by the field lines in Fig. 2). The imaging mechanism can be understood in terms of the antenna properties of the

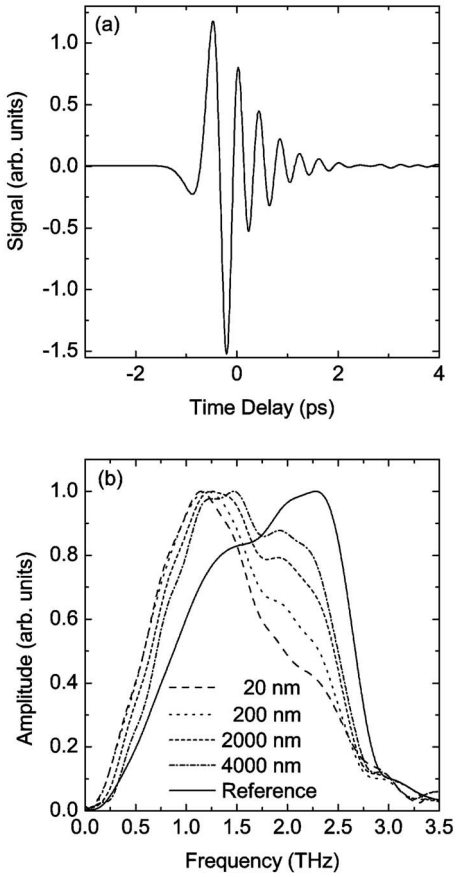

FIG. 1. (a) Transient of a few-cycle terahertz pulse transmitted through the microscope. (b) Normalized near field spectra for different needle surface separations and a reference spectrum of the incident radiation.

tip-surface system.[19,20,33–35] Its relative power dissipation η is

$$\eta_C(\omega)=\frac{RZ_0}{4\pi\left[R^2+\left(\omega L-\frac{1}{\omega C}\right)^2\right]}, \tag{1}$$

where L is the needle's inductance, C is the capacitance of the tip-surface system, and R accounts for dissipative losses as well as for radiation losses of the system.[19]

The intensity and spectral composition of the transmitted radiation are modified by antenna properties of the metallic tip located at the center of the focus. The changes of the dielectric permittivity $\epsilon(\omega,x,y)$ underneath the tip modify the capacitance of the tip-surface system and thus its resonance frequency $\omega_{\text{res}}\approx1/\sqrt{LC}$. This leads to a spectral shift of the transmitted signal, similar to the one in Fig. 1(b). With the exception of the data in Fig. 1(b), all other results presented in this paper were obtained by recording the peak amplitude of the terahertz field transients, i.e., by using the full bandwidth of the impinging terahertz radiation. The terahertz resonance of the tip-surface system usually has a frequency lower than the center frequency of the incident radiation. As a result, an increase of the dielectric constant results in an increased transmission through the microscope head. In our experiments, the near field contribution is measured as a minute change (typically 0.3%) of the transmitted terahertz

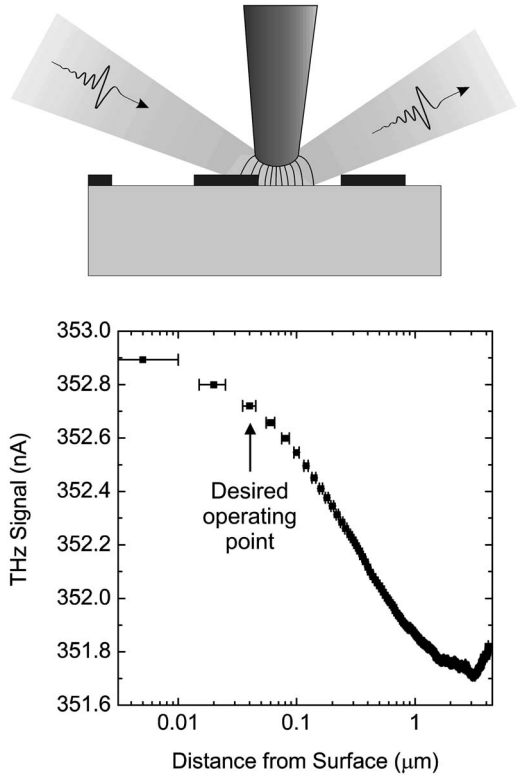

FIG. 2. Schematic of the near field microscope head (top) and experimental data on the transmitted terahertz signal in dependence on the tip-sample separation (bottom).

signal. Two-dimensional imaging is achieved by moving the sample with respect to the incident beam and to the metal tip with a two-dimensional piezostage (Hera P-621.2CL, Physik Instrumente GmbH & Co. KG) operated in closed-loop mode.

Previous investigations have shown that the finest achievable resolution is comparable to the metal tip's apex radius.[22] Most applications require submicron resolution and thus tips with a radius smaller than 1 μm. Additionally, a cone angle of about 16° provides a good coupling to the incident radiation. We fabricate the tungsten probes from 200 or 500 μm thick polycrystalline tungsten wires by electrochemical etching in 1*M* NaOH solution.[36,37] Reproducible tip angles are achieved by immersing and extricating the wire at a frequency of about 0.1 Hz. Typical apex diameters are between 0.2 and 1 μm. Annealing of the tips in a high vacuum chamber at 1300 K removes oxides and increases the hardness of the tip.[38]

Figure 2(b) shows the terahertz amplitude transmitted through the microscope in dependence on the tip-sample separation. In this measurement, the surface contact was determined by the onset of a nonlinear shear force between tip and surface and the distance Δz was measured with a calibrated piezo. The data indicate that an operating point of about 20 nm above the surface is desirable. At this distance, the slope of the curve is close to its maximum value. Hence, a change of the tip-sample distance, or a change of the tip-surface capacitance in general, causes a maximized change of the transmitted signal. Distances smaller than 20 nm are difficult to maintain when scanning topographically uneven

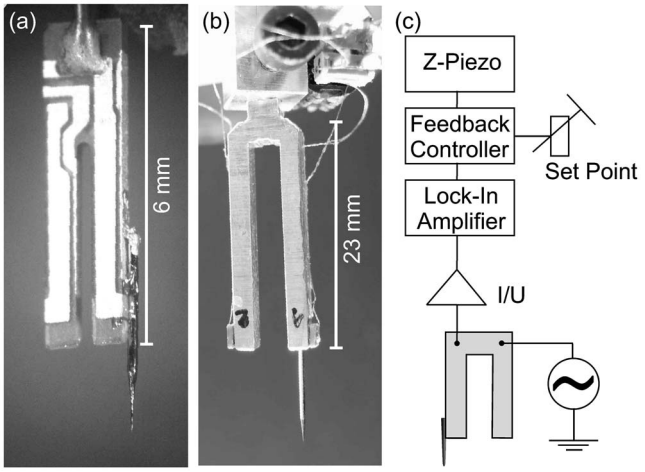

FIG. 3. (a) Quartz tuning fork, (b) aluminum tuning fork, and (c) block diagram of the control loop. The tuning forks are loaded with tungsten wires having thicknesses of 200 and 500 μm for the quartz fork and the aluminum fork, respectively.

surfaces at high speed. The figure also illustrates a major challenge in apertureless terahertz microscopy: During imaging, the tip has to be held at constant height over the surface. Fluctuations on a scale of tens of nanometers would cause a noise level, which would make terahertz microscopy nearly impossible.

B. Shear force control

Shear force control of the tip-surface distance is achieved utilizing quartz tuning forks as well as aluminum forks (Fig. 3). The quartz tuning forks are standard 32.7 kHz devices as used in conventional quartz watches. The tungsten needles are glued with epoxy resin to one of the levers. Applying a high-frequency bias to the two terminals of the fork drives the oscillation of the prongs. The oscillation amplitude is proportional to the amplitude of the drive current, which is measured by a lock-in amplifier. A typical resonance curve is shown in Fig. 4. The resonance is shifted from 32.7 to about 25 kHz due to the load of the tungsten needle. Additionally,

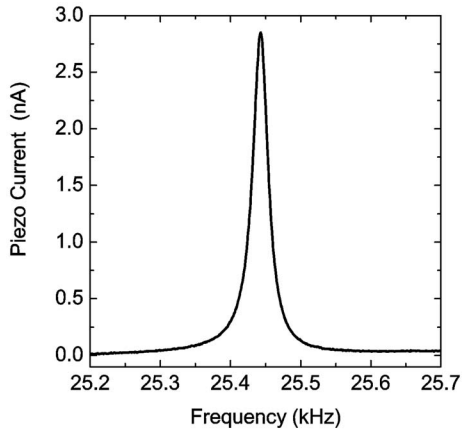

FIG. 4. Frequency dependence of the drive current at the first resonance of a commercial quartz tuning fork. The fork was loaded with a tungsten tip having a diameter of 200 μm and a length of about 5 mm.

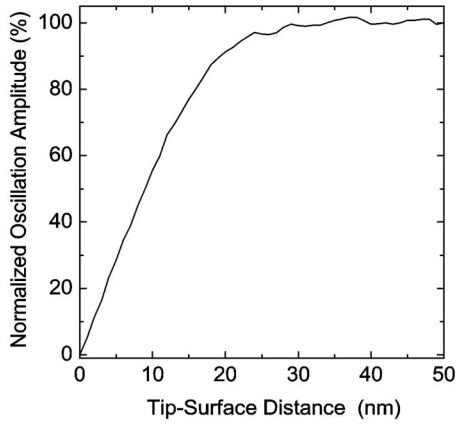

FIG. 5. Normalized amplitude of the piezoelectric current of the aluminum tuning fork in dependence on the tip-surface distance.

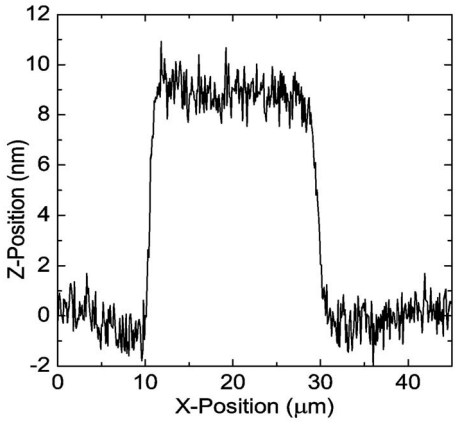

FIG. 6. Topographic profile of a chromium structure on glass recorded by shear force microscopy. The chromium line has a width of 20 μm and a nominal height of 8 nm.

the quality factor of the resonance decreases by more than one order of magnitude when the tuning forks are loaded with a tungsten needle of 0.25 mm radius.

Terahertz microscopy requires tungsten needles that protrude several millimeters over the end of the tuning fork in order to achieve reproducible antenna properties of the tip. Such heavy loads deteriorate the oscillation characteristics of the miniature quartz forks. Much higher loads can be applied to aluminum tuning forks as illustrated in Fig. 3(b). Their size exceeds that of commercial quartz forks by a factor of about 4. The oscillation of the tuning fork is driven by one miniature piezoplate (type c255, PI Ceramic GmbH) glued to the end of one prong. A second piezo is glued to the other prong and is used as readout of the oscillation. The resonance of the lowest acoustic mode is typically at about 10 kHz but higher modes can be found up to frequencies of 100 kHz. For terahertz microscopy, we use resonances of the aluminum tuning fork at about 30 kHz. Typical quality factors are $Q \approx 400$ even when attaching metal tips of 0.5 mm diameter and a lengths of up to 10 mm. A further advantage of the aluminum forks is that it is easy to achieve a galvanic insulation between the piezos and the tungsten tip. This is necessary for electromodulation techniques, where an ac bias is applied between sample and tip in order to sense minute charge carrier distributions.[39]

When the tip approaches the surface, the oscillation amplitude of the tuning fork decreases as shown in Fig. 5. Even when the tip has contact with the surface, the tuning fork performs an oscillation, although with strongly reduced amplitude. In our data, we define the contact to occur when the force on the tip starts changing nonlinearly with any further approach to the surface. This allows us to determine the distance with an accuracy of ±3 nm, which is much smaller than the desired value of 20 nm as discussed above.

The monotonous increase of the oscillation amplitude with distance (Fig. 5) allows for maintaining a constant height of the probe over the sample with the help of a proportional/integral feedback control [Fig. 3(c)]. We use a constant drive frequency for the tuning forks, while the amplitude of the oscillation is monitored by the lock-in amplifier (EG&G 5210). The analog output of the lock-in amplifier provides the input signal for the commercial proportional/integral feedback controller (RHK STM 100) that corrects the tuning fork's position with a time constant of about 5 ms in order to ensure a constant oscillation amplitude. Choosing an amplitude set point of, e.g., 80% of the amplitude of the totally retrieved needle allows for maintaining a constant tip-sample distance of approximately 20 nm.

The tuning fork is moved in the z direction with a linear piezoactuator (P-841.10, Physik Instrumente GmbH & Co. KG). The piezo has a scan range of 15 μm and its calibrated sensor provides positional data with subnanometer resolution. Reading out this sensor provides the topographic data of the sample as it is done in shear force microscopy.

The drive frequency of the tuning fork is set to a value, which is about 10 Hz below the eigenfrequency of the loaded tuning fork (Fig. 4). Typical driving voltages are of the order of $V_{pp}=0.3$ V for the quartz tuning forks and result in currents of several nanoamperes that can be detected with signal to noise ratios exceeding 1000 $\sqrt{\text{Hz}}$. Interferometric measurements carried out by Grober *et al.* showed that the oscillation amplitude scales to the current amplitude with a proportionality factor of $\beta_{\text{quartz}}=0.505$ m/A.[40] Assuming this value for our quartz tuning forks, we conclude that the deflection of the probing tip is about 1.5 nm and thus far below the lateral resolutions that can be achieved in terahertz microscopy. For the aluminum forks, we deduced $\beta_{\text{Al}}=1.8$ m/A by measuring the oscillation amplitude with an interferometer. Typical driving voltages for the aluminum tuning forks are about $V_{pp}=1$ V leading to oscillation amplitudes of about 1 nm.

III. RESULTS

One central question is whether tip-surface distances of the order of 20 nm can be maintained during imaging. Shear force microscopy on a well defined surface structure provides insight. Figure 6 shows the profile of a chromium line on glass, recorded by SFM. According to the fabrication process of the structure, the width of the line is 20 μm and the nominal height is 8 nm. Both the line width and the height of the structure are reproduced by the SFM data. The lateral resolution is about 1 μm, which is comparable to the radius

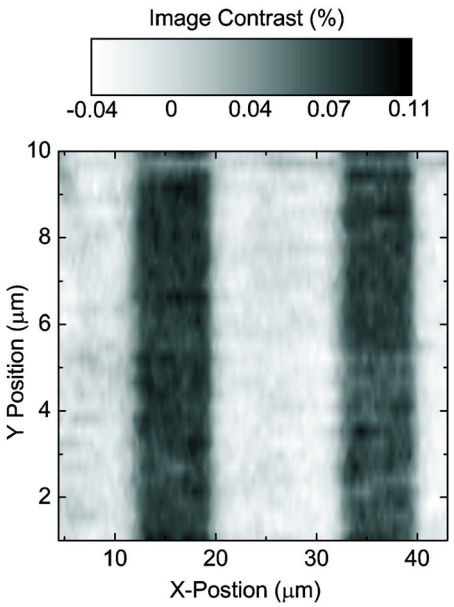

FIG. 7. (Color online) Terahertz image of a grating made of cresol resin. The grating lines have a width of 12 μm and a height of 250 nm. The integration time per data point was 13.3 s.

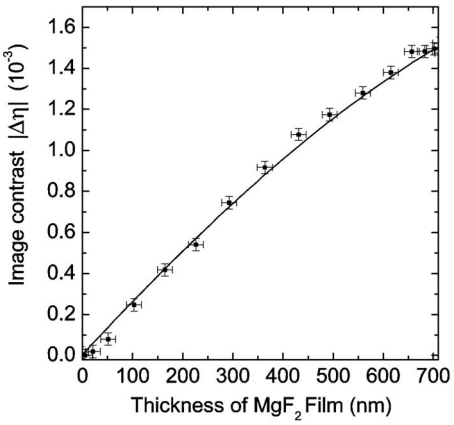

FIG. 8. Absolute change of the image contrast depending on the thickness of the MgF_2 layer (dots) and least mean squares fit based on Eq. (1) (solid line).

of the tungsten tip used in this experiment. From the fact that the height of the line is reproduced, we conclude that the distance between tip and sample is on a comparable scale. Much more important for terahertz microscopy is the rms noise of the tip's z position, which is about 1 nm at a time constant of 4 ms. According to the data shown in Fig. 2, such a noise level of the z position has only a marginal impact on the noise of the terahertz image contrast.

Two mechanisms contribute to the damping of the tuning fork's oscillation when the tip approaches the surface: (i) the van der Waals forces between tip and sample[28] and (ii) damping due to the viscous friction of the needle in a several nanometer thick water layer that covers most surfaces under ambient conditions.[41] Many terahertz experiments are performed at vacuum pressures below 10 mbars in order to eliminate the absorption of terahertz radiation by air moisture. Down to pressures of 0.02 mbar, we found no significant changes in the response of the SFM, which illustrates the general applicability of the approach. Under vacuum conditions, the quality factors of the tuning forks increase because of the reduced friction in air.

The fact that the tip is always held at a distance of about 20 nm allows for terahertz microscopy of soft structures. Figure 7 shows a terahertz micrograph of an organic grating structure made of cresol resin on gold. The cresol resin grating lines have a width of 12 μm, a separation of 8 μm, and a height of about 250 nm. The terahertz image reproduces the structure's width and spacing with a spatial resolution of about 1 μm. The image contrast is about 10^{-3}, and the rms noise of the total terahertz signal is about 4.8×10^{-4} $\mathrm{Hz}^{-1/2}$. Despite the low permittivity of the cresol resin ($\epsilon\approx1.36$), the structure is resolved with a signal to noise ratio of about 7, which required a total integration time of 17 h for the 130×33 data points. Such long integration times are only possible with an active feedback control such as described above. As a result, much more detailed terahertz images are possible, which is evident when comparing the image of Fig. 7 with previous data recorded on a similar structure without shear force control.[19]

The long integration times required for recording terahertz images set limitations for practical applications, in particular, for microscopy on structures with low image contrast. For imaging topographic properties of the sample, established techniques such as AFM or even optical microscopy are more convenient. This should not distract from the unprecedented capability of terahertz microscopy: It provides the local high-frequency permittivity $\epsilon(\omega,x,y)$ on submicron scales. As shown by Eq. (1), the dissipation efficiency of the probe depends on the tip-surface capacitance and thus on the sample's high-frequency dielectric permittivity. However, further quantities such as the inductance or the input resistance contribute to the η. This hinders the direct determination of $\epsilon(\omega,x,y)$ from the experimental data. Therefore, a calibration with a material of known ϵ is useful.

One suitable material for calibration is magnesium fluoride, which exhibits a constant dielectric permittivity $\epsilon_{MgF_2}=5.5$ up to frequencies of about 5 THz.[42] We fabricated on a gold surface a 70 μm long MgF_2 layer, which has a continuously increasing thickness from 0 to 700 nm. The purpose of this wedge is that it decreases in a controlled manner the capacitance formed by the apex of the tip and the gold surface. Figure 8 illustrates the dependence of the image contrast on the thickness of the MgF_2.

The solid line in Fig. 8 shows a calculation that considers the decrease of the capacitance with increasing thickness of the MgF_2. The precise shape of the individual tips is unknown. Therefore, we approximate the capacitance between the needle's apex and the gold substrate by that of a parallel plate capacitor. A fit to the experimental data provides the properties of the sampling tip such as apex size and the input resistance.[43] The obtained parameters are nearly identical to those found in previous work.[19,39] The agreement between terahertz data and calculated data of Fig. 8 indicates that the local dielectric permittivity $\epsilon(\omega,x,y)$ can be measured with extreme subwavelength resolution. Terahertz microscopy is a unique technique providing this insight. Besides this, it is

also worth mentioning that terahertz microscopy is a contactless technique which does not perturb, for instance, the electronic properties of the structure under investigation. This suggests future applications of THz-ANSOM for the characterization of nanostructures or of isolated quantum systems, which are sensitive to external probes, such as, for instance, electrical leads.

IV. CONCLUSION

Apertureless terahertz microscopy with extreme subwavelength resolution requires an active feedback control for maintaining a constant distance between scanning tip and sample. Shear force control is a suitable technique, which is not limited to conductive specimen and can even be applied on soft matter samples. Both commercial quartz tuning forks and miniature aluminum tuning forks allow for maintaining a distance of about 20 nm. With shear force control, terahertz microscopy provides the pure dielectric image contrast. This paves the way for absolute measurements of the complex permittivity on extreme subwavelength dimensions. The fact that the tip-surface distance can be held constant over hours allows for the acquisition of high quality terahertz images even of soft matter.

ACKNOWLEDGMENTS

The authors acknowledge assistance by Florian Kuchler and fruitful discussions with Christian Schiller and Franz Giessibl. The research is supported by the DFG (KE 516/1-1) and by the German Excellence Initiative via the Nanosystems Initiative Munich (NIM).

[1] D. M. Mittleman, R. H. Jacobsen, R. Neelamani, R. G. Baraniuk, and M. C. Nuss, Appl. Phys. B: Lasers Opt. **67**, 379 (1998).
[2] G. Mouret, W. Chen, D. Boucher, R. Bocquet, P. Mounaix, and D. Lippens, Opt. Lett. **24**, 351 (1999).
[3] M. Walther, P. Plochocka, B. Fischer, M. Helm, and P. U. Jepsen, Biopolymers **67**, 310 (2002).
[4] P. F. Taday, I. V. Bradley, D. D. Arnone, and M. Pepper, J. Pharm. Sci. **92**, 831 (2003).
[5] M. van Exter and D. Grischkowsky, Phys. Rev. B **41**, 12140 (1990).
[6] R. Kersting, R. Bratschitsch, G. Strasser, K. Unterrainer, and J. N. Heyman, Opt. Lett. **25**, 272 (2000).
[7] B. B. Hu and M. C. Nuss, Opt. Lett. **20**, 1716 (1995).
[8] Q. Wu, T. D. Hewitt, and X.-C. Zhang, Appl. Phys. Lett. **69**, 1026 (1996).
[9] D. M. Mittleman, S. Hunsche, L. Boivin, and M. C. Nuss, Opt. Lett. **22**, 904 (1997).
[10] B. Ferguson, S. Wang, D. Gray, D. Abbot, and X.-C. Zhang, Opt. Lett. **27**, 1312 (2002).
[11] S. Hunsche, M. Koch, I. Brener, and M. C. Nuss, Opt. Commun. **150**, 22 (1998).
[12] Q. Chen, Z. Jiang, G. X. Xu, and X.-C. Zhang, Opt. Lett. **25**, 1122 (2000).
[13] O. Mitrofanov, M. Lee, J. W. P. Hsu, I. Brener, R. Harel, J. F. Federici, J. D. Wynn, L. N. Pfeiffer, and K. W. West, IEEE J. Sel. Top. Quantum Electron. **7**, 600 (2001).
[14] H. A. Bethe, Phys. Rev. **66**, 163 (1944).
[15] J. E. Wessel, J. Opt. Soc. Am. B **2**, 1538 (1985).
[16] M. Specht, J. D. Pedarnig, W. M. Heckl, and T. W. Hänsch, Phys. Rev. Lett. **68**, 476 (1992).
[17] B. Knoll and F. Keilmann, Opt. Commun. **182**, 321 (2000).
[18] N. C. J. van der Valk and P. C. M. Planken, Appl. Phys. Lett. **81**, 1558 (2002).
[19] H.-T. Chen, S. Kraatz, G. C. Cho, and R. Kersting, Phys. Rev. Lett. **93**, 267401 (2004).
[20] K. Wang, D. M. Mittleman, N. C. J. van der Valk, and P. C. M. Planken, Appl. Phys. Lett. **85**, 2715 (2004).
[21] P. C. M. Planken, C. E. W. M. van Rijmenam, and R. N. Schouten, Semicond. Sci. Technol. **20**, 121 (2005).
[22] H.-T. Chen, R. Kersting, and G. C. Cho, Appl. Phys. Lett. **83**, 3009 (2003).
[23] G. C. Cho, H.-T. Chen, S. Kraatz, N. Karpowicz, and R. Kersting, Semicond. Sci. Technol. **20**, 286 (2005).
[24] R. Kersting, H.-T. Chen, N. Karpowicz, and G. C. Cho, J. Opt. A, Pure Appl. Opt. **7**, 184 (2005).
[25] K. Karrai and R. D. Grober, Appl. Phys. Lett. **66**, 1842 (1995).
[26] W. H. J. Rensen, N. F. van Hulst, A. G. T. Ruiter, and P. E. West, Appl. Phys. Lett. **75**, 1640 (1999).
[27] F. J. Giessibl, Appl. Phys. Lett. **73**, 3956 (1998).
[28] F. J. Giessibl, Rev. Mod. Phys. **75**, 949 (2003).
[29] R. Kersting, K. Unterrainer, G. Strasser, H. F. Kauffmann, and E. Gornik, Phys. Rev. Lett. **79**, 3038 (1997).
[30] M. P. Hasselbeck, D. Stalnaker, L. A. Schlie, T. J. Rotter, A. Stintz, and M. SheikBahae, Phys. Rev. B **65**, 233203 (2002).
[31] For this purpose, terahertz transients were recorded for the respective tip-sample separations and for the needle retrieved to 14 μm distance. Figure 1(b) shows the Fourier amplitudes of the differential time domain signal, since the bare terahertz transients just differ by $\leqslant 1\%$ due to the transmission design of our experiment.
[32] Q. Wu and X.-C. Zhang, Appl. Phys. Lett. **67**, 3523 (1995).
[33] K. Wang and D. M. Mittleman, Nature (London) **432**, 376 (2004).
[34] M. Walther, G. S. Chambers, Z. Liu, M. R. Freeman, and F. A. Hegmann, J. Opt. Soc. Am. B **22**, 2357 (2005).
[35] A. J. L. Adam, N. C. J. van der Valk, and P. C. M. Planken, J. Opt. Soc. Am. B **24**, 1080 (2007).
[36] A. J. Melmed, J. Vac. Sci. Technol. B **9**, 601 (1991).
[37] J. P. Ibe, P. P. Bey, Jr., S. L. Brandow, R. A. Brizzolara, N. A. Burnham, D. P. DiLella, K. P. Lee, C. R. K. Marrian, and R. J. Colton, J. Vac. Sci. Technol. A **8**, 3570 (1990).
[38] I. Ekvall, E. Wahlström, D. Claesson, H. Olin, and E. Olsson, Meas. Sci. Technol. **10**, 11 (1999).
[39] F. Buersgens, R. Kersting, and H.-T. Chen, Appl. Phys. Lett. **88**, 112115 (2006).
[40] R. D. Grober, J. Acimovic, J. Schuck, D. Hessman, P. J. Kindlemann, J. Hespanha, A. S. Morse, K. Karrai, I. Tiemann, and S. Manus, Rev. Sci. Instrum. **71**, 2776 (2000).
[41] S. Davy, M. Spajer, and D. Courjon, Appl. Phys. Lett. **73**, 2594 (1998).
[42] E. D. Palik, *Handbook of Optical Constants of Solids II* (Academic, New York, 1991).
[43] The relation used here is $|\Delta\eta| = |\eta(\omega_0, C_{\text{air}}) - \eta(\omega_0, C_{\text{air,MgF}_2})|$, where ω_0 is the terahertz center frequency, C_{air} is the parallel plate capacitance of the tip-surface system with a 20 nm air gap, and $C_{\text{air,MgF}_2}$ is the series capacitance of the tip-surface and the MgF_2 layer capacitance for variable MgF_2 thicknesses.